Desalination and Water Treatment
www.deswater.com

doi: 10.1080/19443994.2013.799049

52 (2014) 3392–3402
April

Taylor & Francis
Taylor & Francis Group

Enhanced photocatalytic activity of titanium dioxide by β-cyclodextrin in decoloration of Acid Yellow 99 dye

Sakthivel Pitchaimuthu, Subramanian Rajalakshmi, Nagarathinam Kannan, Ponnusamy Velusamy*

Centre for Research and Post Graduate Studies in Chemistry, Ayya Nadar Janaki Ammal College, Sivakasi 626 124, Tamilnadu, India
Tel. +91 9443572149; Fax: +91 04562 254970; email: velusamyanjac@rediffmail.com

Received 22 January 2013; Accepted 17 April 2013

ABSTRACT

Photocatalytic decoloration of Acid Yellow 99 dye by TiO_2 has been investigated under different experimental conditions. Addition of β-Cyclodextrin on TiO_2 enhanced the photoactivity of TiO_2 in AY99 degradation. Optimal experimental conditions on catalyst amount, pH value, illumination time, and dye concentration have been determined. The mineralization of AY99 has been confirmed by Chemical Oxygen Demand measurements. The higher photoactivity of TiO_2-β-CD/visible light system than TiO_2/visible light system can be ascribed due to the ligand to metal charge transfer from β-CD to Ti^{IV} located in an octahedral coordination environment. The complexation patterns have been confirmed with UV–Visible and FT-IR spectral data. The interactions between TiO_2 and β-CD have been characterized by Field Emission Scanning Electron Microscopy, X-ray powder diffraction analysis, and UV–Visible diffuse reflectance spectroscopy.

Keywords: Acid Yellow 99 dye; β-Cyclodextrin; TiO_2; Photocatalytic decoloration; COD

1. Introduction

Photocatalytic processes of organic pollutants under various light sources (i.e. UV, Visible, and Solar) have attracted increasing attention during the past two decades, because of their greater potential for converting photon energy into chemical energy [1]. The photocatalysis mechanism of wide band gap semiconductor involving the excitation of electrons from valence band of semiconductors (e.g. TiO_2 and ZnO) to conduction band (CB) and thus forming electron-hole pairs are responsible for the photocatalytic activity of the semiconductors simultaneously [2]. During the course of the reaction, a variety of reactive oxidation species (ROSs) are formed which oxidize the organic compounds [3,4] especially organic dyes. A major limitation for achieving high photocatalytic efficiency is the quick recombination of photo-generating electron-hole pairs, which is faster than the surface redox reactions. This leads to serious reduction of quantum efficiency of photocatalysis [1,5]. Moreover, the wide bandgap semiconductors can only be excited by UV light which occupies less than 10% of the total energy of the solar radiation [6,7]. The development of

*Corresponding author.

This article was originally published with an error in the order of authors' names. This version has been corrected. Please see Corrigendum [10.1080/19443994.2013.813620]

visible-light-driven photocatalysts with high energy transfer efficiency has become one of the most challenging tasks these days. Thus a number of efforts have been employed to inhibit the recombination of electron-hole pairs and improve charge transport via coupling the wide band gap semiconductor photocatalysts with other materials, such as semiconductor/noble-metal composite, quantum dot-semiconductor composite, C–N doped semiconductor, carbon nanotubes, or fullerene (C_{60})-semiconductor composites [5,8–12].

Cyclodextrins (CDs) are non-reducing cyclic maltooligosaccharides produced from of six to eight α-D-glucose units connected through glycosidic α-1,4 bonds, which are composed of hydrophobic internal cavity and hydrophilic external surface. CDs can form inclusion complexes with organic pollutants and organic pesticides to reduce the environmental impact of the chemical pollutants. β-Cyclodextrin (β-CD) contains seven α-D-glucose units connected through glycosidic α-1,4 bonds, is a sophisticated material for enhancing the photocatalytic activity of TiO_2. CD modified semiconductor nanocomposites have attracted renewed interest since, Willner and his colleagues who observed that β-CD could stabilize TiO_2 colloids and facilitate interfacial electron transfer processes [13–15]. Excellent literatures have been published to prove the effect of β-CD on TiO_2 photochemical properties [16–20]. All previous works suggest that β-CD plays electron-donating and hole-capturing roles when linked to TiO_2 colloids, which leads to charge-hole recombination restriction and photocatalytic efficiency enhancement. Through literature, survey reveals the stimulative effect of CD on the photocatalytic degradation of organic pollutants in TiO_2 suspensions [21–26].

Large amount of dyes are annually used in textile, cosmetics, food, pharmaceutical, and paper industries [27]. Azo dyes constitute largest and the most important classes of commercial dyes [28]. The fixation degree of azo dyes to fabrics is not complete, resulting in the contamination of the effluents in wastewater [29,30]. Azo dyes are characterized by the existence of N=N bonds and the bright color is due to the azo bonds and chromospheres [31]. Furthermore, azo dyes also affect photochemical activities in aquatic systems by reducing light penetration. The removal of azo dyes is an important process, because many azo dyes are toxic to aquatic organisms [32,33]. For these reasons we chose an azo dye, Acid Yellow 99 (AY99) dye as a model dye pollutant to investigate the photocatalytic decolorability of TiO_2 by addition of β-CD under visible light radiation. The results are well documented and a suitable mechanism has been proposed.

2. Experimental

2.1. Materials

The commercial organic dye AY99 ($\lambda_{max} = 445$ nm) obtained from Loba Chemie was used as such. The semiconductor photocatalyst TiO_2 was purchased from Merck Chemicals. β-CD was received from Himedia chemicals. All other chemicals were of the Analytical grade, received from Merck and used without further purification. Double distilled water was used throughout this study for the preparation of all the experimental solutions. The physical properties and structures of AY99 dye and β-CD are shown in Table 1.

2.2. Characterization

FE-SEM was used to investigate the morphology of the samples β-CD, TiO_2, and TiO_2-β-CD. FE-SEM images were obtained on a Carl ZEISS (ΣIGMA Series, Germany) microscope taken at an accelerated voltage of 2 kV. X-ray diffraction patterns of powdered samples were recorded with a high resolution powder X-ray diffractometer model RICH SIERT & Co with CuK_α radiation as the X-ray source ($\lambda = 1.5406 \times 10^{-10}$ m). UV–Vis diffuse reflectance spectra were recorded on a Shimadzu 2550 UV–Vis diffuse reflectance spectrophotometer with $BaSO_4$ as the background between 200 and 700 nm. UV–Visible spectra were recorded by a UV–Visible spectrophotometer (Shimadzu UV-1700) and the scan range was from 400 to 700 nm. FT-IR spectra were recorded using FT-IR spectrometer (Shimadzu model 8400S) in the region 4,000–400 cm^{-1} using KBr pellets.

2.3. Experimental conditions

Photocatalytic decoloration experiments were carried out under visible light irradiation. AY99 dye solutions containing the photocatalysts of either TiO_2 or TiO_2-β-CD were prepared. The pH values of dye solutions were adjusted using digital pen pH meter (Hanna Instruments, Portugal) depending on desired values with HCl and NaOH solution as their effect on the adsorption surface properties of TiO_2 is negligible [34]. The pH of the dye solutions was adjusted before irradiation process and it was not controlled during the course of the reaction. Prior to irradiation TiO_2 suspensions were kept in dark for 10 min, to attain adsorption-desorption equilibrium between dye and TiO_2/visible light system. Heber Annular type visible (500 W, OSRAM) photoreactor was used as light source in the central axis. The reaction vessels were taken out at different intervals of time and the

Table 1
Physical properties of AY99 dye and β-CD

Name	Acid Yellow 99 dye	β-Cyclodextrin
Molecular formula	$C_{16}H_{13}CrN_4NaO_8S$	$C_{42}H_{70}O_{35}$
Molar weight	496.35	1135.0
Appearance	Yellow powder	White powder
pH	5.4 (acidic dye)	–
λ_{max}	445 nm	–
Structure	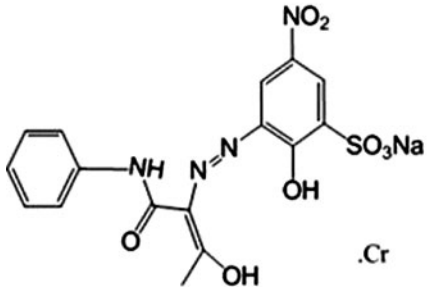	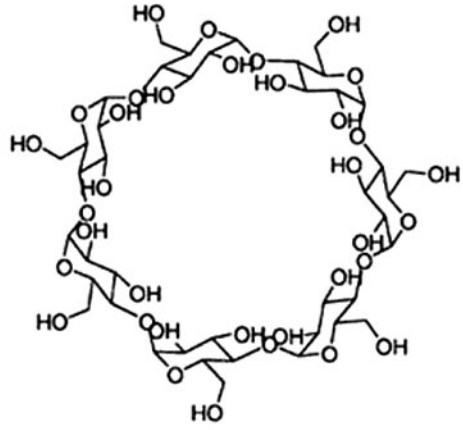

solutions were centrifuged. The supernatant liquid was collected for the determination of concentrations for the remaining dye by measuring its absorbance (at $\lambda_{max} = 445$ nm) with visible spectrophotometer (ELICO, Model No. SL207). In all the cases, exactly 50 mL of the reactant solution was irradiated with the required amount of photocatalysts.

By keeping the concentrations of AY99 dye-β-CD constant with the molar ratio of 1:1, the effects of the other experimental parameters on the rate of photocatalytic decoloration of AY99 dye solutions were investigated. The natural pH of AY99 dye solution was 5.4 and the irradiation time was fixed as 120 min.

2.4. Determination of chemical oxygen demand (COD)

Exactly 50 mL of the sample was taken in a 500 mL round bottom flask with 1 g of mercuric sulphate. Slowly, 5 mL of silver sulphate reagent (prepared from 5.5 g silver sulphate per kg in concentrated sulphuric acid) was added to the solution. Cooling of the mixture is necessary to avoid possible loss of volatile matters if any, while stirring. Exactly 25 mL of 0.041 M potassium dichromate solution was added to the mixture slowly. The flask was attached to the condenser and 70 mL of silver sulphate reagent was added and allowed to reflux for 2 h. After refluxion, the solution was cooled at room temperature. Five drops of Ferroin indicator was added and titrated against a standard solution of ferrous ammonium sulphate (FAS) until the appearance of the first sharp color change from bluish green to reddish brown. The COD values can be calculated in terms of oxygen per litre in milligram (mg O_2/l) using the following Eq. (1) [35].

$$\text{COD mg}\,O_2/l = (B - A)\,M\,8,000/S \quad (1)$$

where B is the millilitre of FAS consumed by $K_2Cr_2O_7$, A is the millilitres of FAS consumed by $K_2Cr_2O_7$ and AY99 dye mixture, M is the molarity of FAS and S the volume of the AY99 dye.

2.5. Preparation of TiO_2-β-CD and AY99-β-CD samples for characterisation

In order to study the interaction of β-CD on TiO_2 surface, a suspension containing 2.0 g/L TiO_2 and 10.0 g/L β-CD was magnetically stirred for 24 h, centrifuged, and then the solid phase was collected. After being centrifuged, the solid phase of the suspension was carefully washed with double distilled water until no β-CD was detected in the supernatant liquid by phenolphthalein colorimetry [26]. Eventually, the

TiO_2-β-CD sample was dried at 50°C. The sample prepared in this way was used for Field Emission Scanning Electron Microscopy (FESEM), XRD, and UV-DRS analysis.

For studying the inclusion complex between β-CD and AY99 dye, saturated solution of β-CD in distilled water, equimolar amount of AY99 dye was added and stirred continuously for 24 h and then the complex powder was filtered, washed with diethyl ether to remove uncomplexed AY99 dye, and dried in an air oven at 50°C. The resultant complex obtained was used as such for FT-IR spectral analysis.

3. Results and discussion

3.1. Catalyst characteristics

3.1.1. Field emission scanning electron microscopy

Fig. 1 depicts FESEM micrograph of the bare β-CD, bare TiO_2, and TiO_2-β-CD respectively. Bare CD shows amorphous surface. The surfaces of bare TiO_2 and TiO_2-β-CD exhibit a similar morphology which indicates that there is no change in the lattice structure of TiO_2. However, the outer boundary of the TiO_2-β-CD was distinctly different from TiO_2. This may be due to the aggregation of TiO_2 and β-CD particles as the surfaces of the particles are very loose. This kind of surface structure can provide a better adsorption environment and a more active site for the photocatalytic reaction.

3.1.2. X-ray powder diffraction patterns

The X-ray powder diffraction patterns (PXRD) of bare TiO_2, bare β-CD, and TiO_2-β-CD are presented in Fig. 2(a)–(c). The XRD analysis of TiO_2 reveals that sample exhibits single-phase belongs to anatase-type TiO_2 which is identified by comparing the spectra with the JCPDS file # 21–1,272. Diffraction peaks at 25.38°, 37.9°, 48.07°, 53.94°, and 55.18° correspond to (101), (004), (200), (105), and (211) planes of TiO_2 respectively. The relatively high intensity of the peak

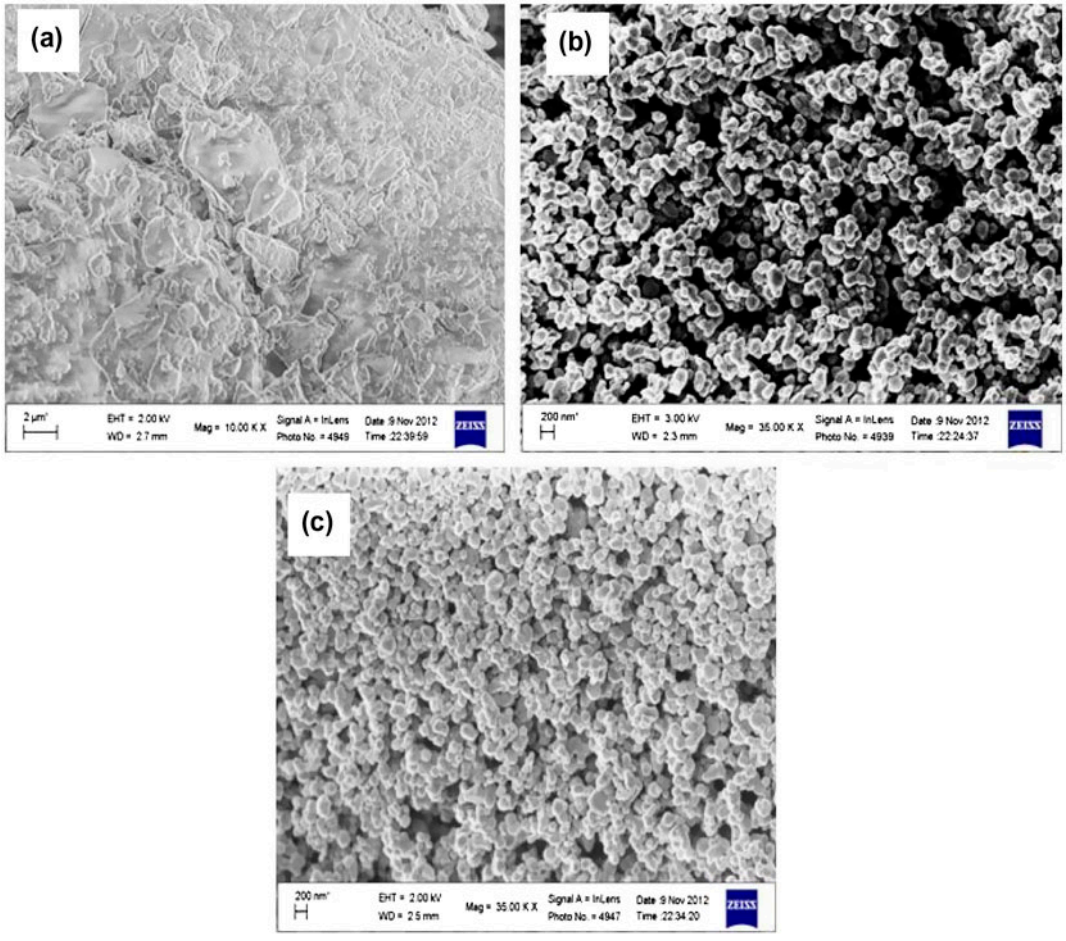

Fig. 1. FESEM images of (a) Bare β-CD (b) Bare TiO_2 (c) TiO_2-β-CD.

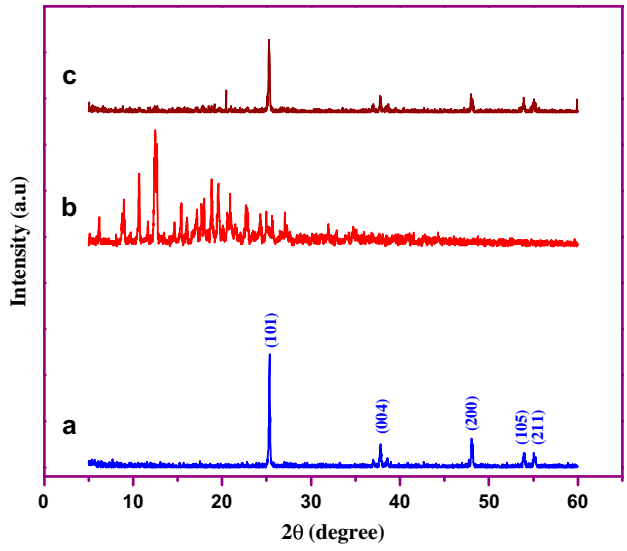

Fig. 2. PXRD of (a) Bare TiO_2 (b) Bare β-CD (c) TiO_2-β-CD.

for (101) plane is an indicative of anisotropic growth which implies a preferred orientation of the crystallites. Addition of β-CD does not cause any shift in peak position of that of TiO_2 phase. The results also demonstrated that the anatase TiO_2 conserved their anatase crystal features. Addition of β-CD causes no effect on the crystalline feature of TiO_2. The same results were also reported by Zhang et al. [24].

3.1.3. UV–Visible diffuse reflectance spectra

The UV–Visible diffuse reflectance spectrum of bare TiO_2 and TiO_2-β-CD are shown in Fig. 3. The reflectance data, F(R) values have been obtained by application of the Kubelka–Munk algorithm. The band gap of the photocatalysts has been deduced from the Tauc plot. Fig. 3 is the plot of $[F(R)\ h\upsilon]^{1/2}$ *vs.* adsorption energy. β-CD modification leads to a significant effect on the optical characteristics of TiO_2. TiO_2-β-CD system has a slightly higher absorption intensity in the visible region compared to the bare TiO_2 Fig. 3 (Inset), this is attributed to the charge transfer from β-CD to Ti^{IV} (i.e. ligand to metal charge transfer located in an octahedral coordination environment. [36–38].

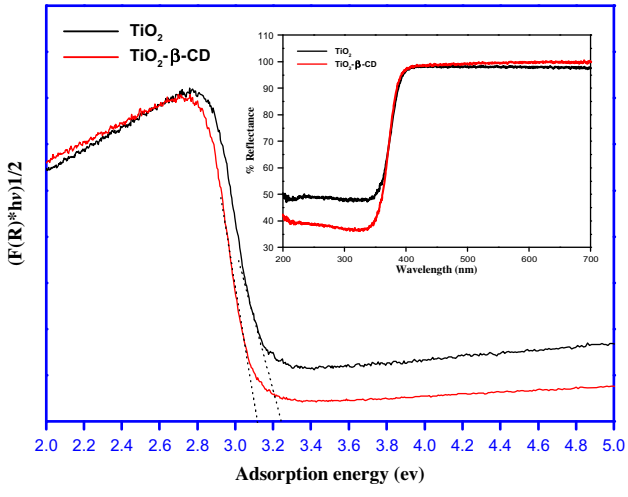

Fig. 3. UV–Visible DRS spectra of Bare TiO_2 and TiO_2-β-CD.

3.1.4. UV–Visible and FT-IR spectral analyses

The molecular structure of β-CD allows various guest molecules with suitable dimensions to form host/guest inclusion complexes. In this study, the inclusion complex between β-CD and AY99 dye was characterized with UV–Visible spectra as given in Fig. 4. Fig. 4 depicts that the absorbance of inclusion complex increases with increasing the concentration of β-CD [23]. In this work, the optimum molar ratio between β-CD and AY99 dye was fixed as 1:1.

Though IR measurements are not employed for detecting inclusion compounds (due to the superposition of host and guest bands), in some cases where the substrate has characterstic absorbance in the regions where β-CD does not absorb, IR spectrum is useful [39]. From the FT-IR spectra in Fig. 5(a)–(d), it was observed that the peaks corresponding to mono-substituted benzene (1,596, 1,544, and 1,514 cm^{-1}) for the AY99 dye molecule (Fig. 5(b)) are present in the

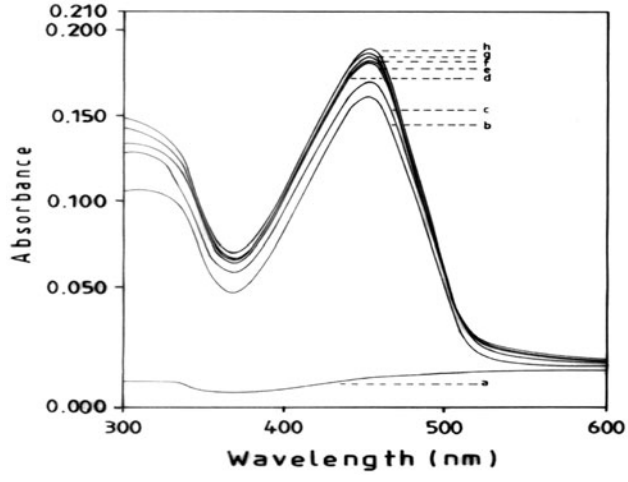

Fig. 4. UV–Visible spectral analysis for the complexation pattern between β-CD and AY99 dye (a) β-CD (b) AY99 dye (c) 1:1 β-CD/AY99 (d) 2:1 β-CD/AY99 (e) 3:1 β-CD/AY99 (f) 4:1 β-CD/AY99 (g) 5:1 β-CD/AY99 (h) 6:1 β-CD/AY99.

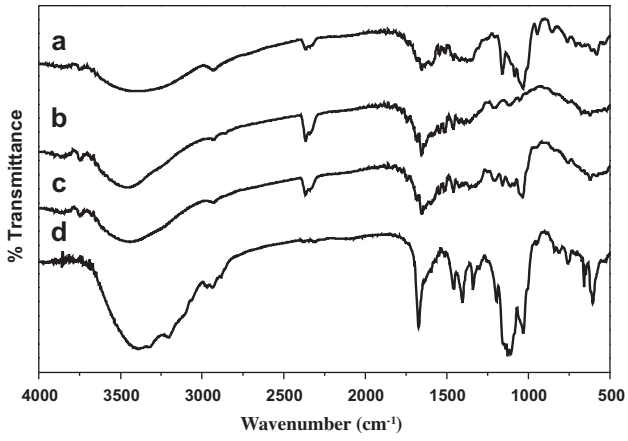

Fig. 5. FT-IR spectral analysis β-CD (b) AY99 dye (c) 1:1 Physical mixture of β-CD and AY99 dye (d) β-CD/AY99 complex.

1:1 physical mixture of β-CD-AY99 dye (Fig. 5(c)), where as it is hidden in the β-CD-AY99 dye 1:1 complex (Fig. 5(d)). Moreover, it contains all the absorption peaks related to β-CD (Fig. 5(a)). It is interesting to note that the spectrum of a physical mixture of β-CD and AY99 dye resembles more of the AY99 dye peaks than that of their complex spectrum. In addition, decrease in intensities of many bands is observed in β-CD-AY99 dye complex spectrum. The complexation between the AY99 dye molecule and β-CD has been proved by the FT-IR spectral data.

3.2. Effect of operational parameters

3.2.1. Effect of initial dye concentration

The photocatalytic decoloration of AY99 dye was carried out at different initial concentrations ranging from 0.806×10^{-5} to 4.835×10^{-5} M in TiO_2/visible light system and TiO_2-β-CD/visible light systems. The percentage removal of AY99 dye was decreased with increasing the concentration of dye. An explanation to this behaviour is that as initial concentration increases, more and more dye molecules are adsorbed on the surface of TiO_2. There are only a fewer active sites for the adsorption of hydroxyl ions, thus reduces the generation of hydroxyl radicals. Further, as the concentration of dye molecules increases, the photons get intercepted before they can reach the catalyst surface. Hence, the absorption of photons by the catalyst decreases and consequently the decoloration rate is reduced [40,41]. The optimum concentration of AY99 dye was fixed as 1.612×10^{-5} M for further studies.

3.2.2. Effect of initial pH

The pH of the solution is one of the main factors which influence the rate of degradation of organic compounds in the photocatalytic processes. It is also an important operational variable in actual wastewater treatment [40]. Acid dyes are also called anionic dyes because of the negative electrical structure of the chromophore. Thus, a negative surface charge does not favor the adsorption of dye anions due to their electrostatic repulsion. Due to the electrostatic attraction of the positively charged catalyst with the ionized sulfonic group of this acidic dye, a higher decoloration rate is obtained. At these pH values, there is also formation of more number of $OH^{\bullet}$ radicals which react with the dye molecules and increase the decoloration level [42]. The uptakes of dye anion are much higher in acidic solutions than those in neutral as well as in alkaline conditions. Photodegradation of AY99 at different pH values from 1 to 11 clearly shows that acceptable results are obtained in acidic solution. As the zero point charge of TiO_2 is 6.8, its surface is presumably positively charged in acidic solution and negatively charged in alkaline solution. For the above reasons, dyes that have negatively charged sulphonyl group in its structure favors adsorption of dye onto the photocatalyst surface in acidic solution and thus the photodegradation efficiency increases effectively. There is also the photocatalytic degradation of AY99 in acidic solutions, which is probably due to the formation of $^{\bullet}OH$ [41,43].

3.2.3. Effect of dose of TiO_2 variation

The influence of the TiO_2 concentration from 0.5 to 3.0 g/L for AY99 dye on the photodecoloration efficiency was investigated. The observed results revealed that the photodecoloration efficiency increases with increase in the TiO_2 concentration. This can be explained in terms of availability of active sites on the catalyst surface, which increases the number of dye molecules adsorbed and the increase in the density of particles in the area of illumination [33]. Hence, the optimum amount of catalyst for photocatalytic decoloration of AY99 dye was found to be 2.0 g/L. All the above process parameters were performed, with this concentration of TiO_2.

3.2.4. Effect of illumination time

Illumination time plays a vital role in the decoloration process of the pollutants. The illumination time was varied from 30 to 180 min. The remaining concen-

tration of the AY99 dye is decreased with an increase in the illumination time. It is observed that nearly 92.8% decoloration of AY99 dye solution was achieved within 180 min.

3.3. Decoloration kinetics

Several experimental results indicate that the degradation rates of the photocatalytic decoloration process of AY99 dye over illuminated TiO_2 is fitted with the pseudo-first order kinetic model AY99 [44,45]. The regression curve of natural logarithm of AY99 concentration *vs* illumination time gives a straight line in both the cases (i.e. TiO_2/visible light system and TiO_2-*β*-CD/visible light system) (Fig. 6). The linearity of plot suggests that the photodecoloration reaction approximately follows the pseudo-first order using the formula,

$$\ln (C_0/C_t) = k_t \quad (2)$$

where C_0 and C_t represent the initial concentration of the corresponding AY99 dye in solution and that of illumination time of t, respectively, and k_t represents the apparent rate constant (min^{-1}).

3.4. Promotion effects of β-CD on the photodecoloration rate

From the observed results, it is clearly understood that the promotion effect of *β*-CD on photodecoloration rate of AY99 dye tend to increase in TiO_2-*β*-CD/visible light system than TiO_2/visible light system (Fig. 7). This suggests that the promotion effects of *β*-CD observed here are not due to a simple extension of the photodecoloration mechanism of AY99 dye in the *β*-CD less reaction solution, but due to the introduction of another mechanism possibly sustained by the high inclusion abilities of *β*-CD, such that they are effectual not only to AY99 dye but also to the radicals generated by the TiO_2. The abilities of *β*-CD for inclusion-trapping of radicals are actually recognized in the case of several reactive radical species [46].

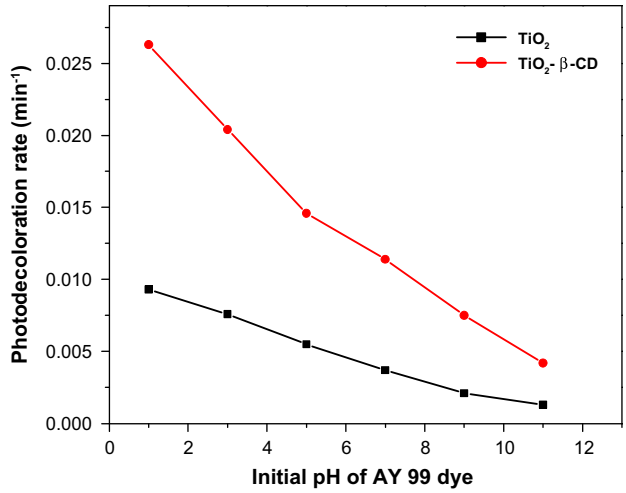

Fig. 7. Photodecoloration rate vs initial pH of AY99 dye.

3.5. Mineralization

β-CD is photochemically stable. It does not undergo degradation under illumination. Hence, the COD corresponds to AY99 dye molecules alone. The

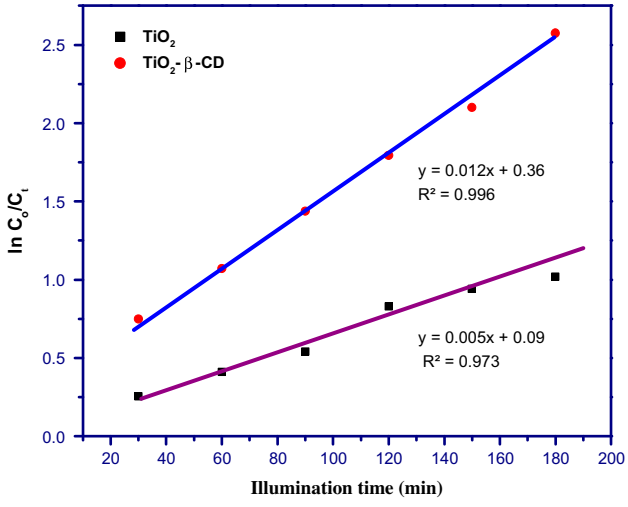

Fig. 6. ln C_0/C_t vs illumination time (min).

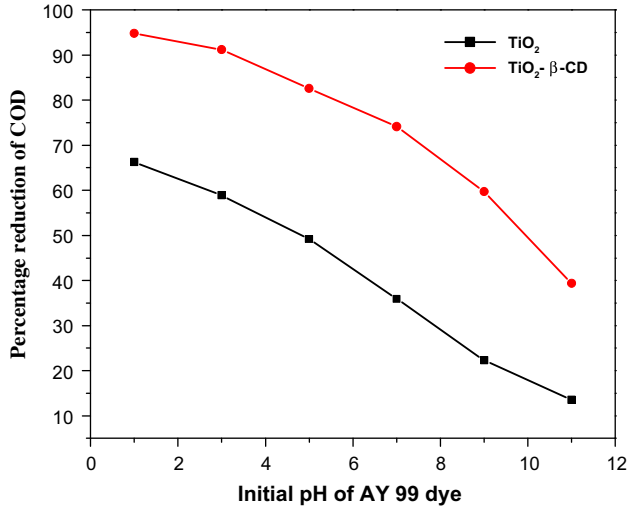

Fig. 8. Percentage reduction of COD vs initial pH of AY99 dye.

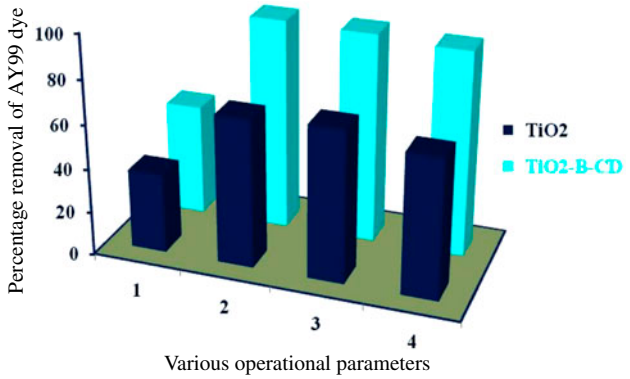

Fig. 9. Various operational parameters vs percentage removal of AY99 dye. where 1=> Effect of initial concentration of AY 99 dye solutions. 2=> Effect of pH variation. 3=> Effect of dose variation. 4=> Effect of irradiation time.

mineralization experiments were carried out at different pH values from 1 to 11. To the AY99 dye solution TiO_2 2 gL^{-1} and aqueous β-CD solution were added. The concentration ratio between β-CD and AY99 dye was made in 1:1 ratio. The photocatalytic procedure was followed, the irradiated samples were collected, and COD values were determined. The obtained results indicate that the percentage reduction of COD decreases with increasing the initial pH of AY99 dye solution (Fig. 8).

Fig. 9 confirms the maximum percentage removal of AY99 with various operational parameters. It is observed that TiO_2-β-CD/visible light system exhibits better photocatalytic decoloration efficiency than that of TiO_2/visible light system.

3.6. Dissociation constant measurements

The dissociation constant (K_D) value for the complexation between β-CD and AY99 dye can be calculated using the Benesi-Hildebrand Eq. (3) [39].

$$([C]\,[S]/\Delta OD) = ([C] + [S]/\Delta\varepsilon) + (K_D/\Delta\varepsilon) \quad (3)$$

where

[C] and [S] represent the concentrations of the β-CD, AY99 dye molecules respectively at equilibrium. ΔOD = the increase in absorption upon addition of β-CD $\Delta\varepsilon$ = the difference in molar extinction coefficients between the bound and the free AY99 dye. K_D = dissociation constant K_D can be obtained from the ratio of the intercept ($K_D/\Delta\varepsilon$) and the slope ($1/\Delta\varepsilon$) from the linear plot of [C] [S]/ΔOD vs {[C] + [S]} (Fig. 10). The determined K_D value is 4.8846×10^{-5} M.

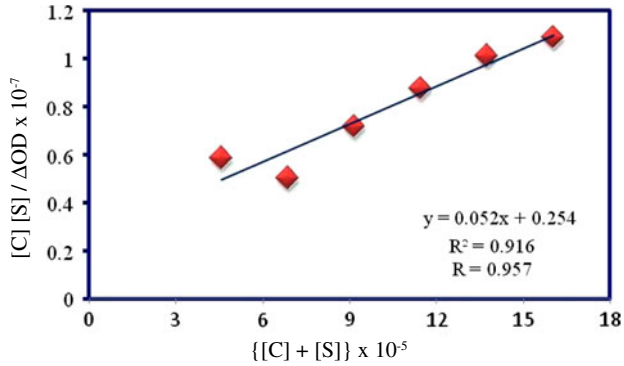

Fig. 10. $\{[C]\,[S]/\Delta OD)\} \times 10^{-7}$ vs $\{[C] + [S]\} \times 10^{-5}$.

Fig. 11 shows spectral irradiance and the transmitted wavelengths of 500 W visible lamp. The calculated adsorption capacity of β-CD onto TiO_2 was 10.75 μM/g calculated by Langmuir isotherm model (Fig. 12).

3.7. Mechanism of the effect of β-CD on photodecoloration

The following reactions (a–k) explain the induced photodecolorisation of AY99 dye by three systems *viz.*

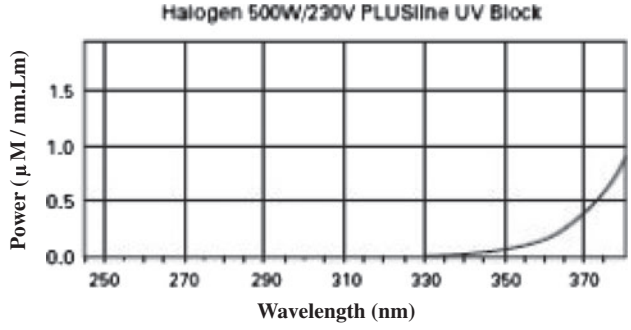

Fig. 11. Spectral irradiance and the transmitted wavelengths of 500 W visible lamp.

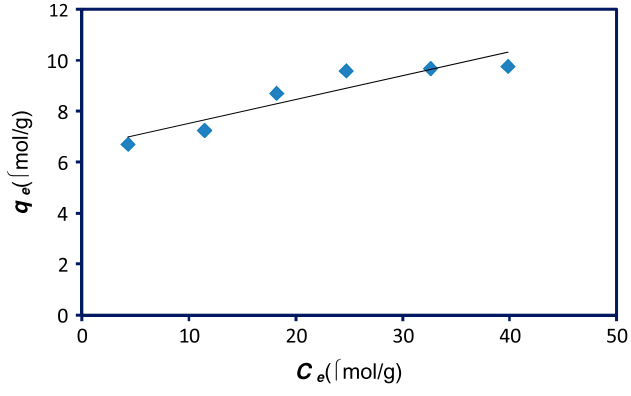

Fig. 12. Langmuir isotherm model.

TiO_2, AY99 dye-β-CD inclusion complex, and TiO_2-β-CD.

$$\text{AY99 Dye} + TiO_2 \rightarrow H_2O + CO_2 + \text{Mineralization products} \quad \text{(a)}$$

$$\beta - CD + TiO_2 \rightarrow TiO_2 - \beta - CD \quad \text{(b)}$$

$$\text{AY99 Dye} + \beta - CD \rightarrow \beta - CD - \text{AY99 Dye} \quad \text{(c)}$$

$$\text{AY99 Dye} + TiO_2 - \beta - CD \rightarrow TiO_2 - \beta - CD - \text{AY99 Dye} \quad \text{(d)}$$

$$TiO_2 - \beta - CD - \text{AY99 Dye} + h\nu \rightarrow TiO_2 - \beta - CD^{\bullet 1}\text{AY99 Dye}^* + TiO_2 - \beta - CD^{\bullet 3}\text{AY99 Dye}^* \quad \text{(e)}$$

$$TiO_2 - \beta - CD - \text{AY99 Dye}^* \rightarrow (e^-)TiO_2 - \beta - CD + \text{AY99 Dye}^{\bullet +} \quad \text{(f)}$$

$$TiO_2 - \beta - CD - \text{AY99 Dye}^* + O_2 \rightarrow TiO_2 - \beta - CD - \text{AY99 Dye} + {}^1O_2 \quad \text{(g)}$$

$$(e^-)TiO_2 - \beta - CD + O_2 \rightarrow TiO_2 - \beta - CD + {}^{\bullet}O_2^- \quad \text{(h)}$$

$$\text{AY99 Dye}^{\bullet +} \rightarrow \text{Products} \quad \text{(i)}$$

$$\text{AY99 Dye} + {}^1O_2 \rightarrow \text{Products} \quad \text{(j)}$$

$$\text{AY99 Dye} + {}^{\bullet}O_2^- \rightarrow \text{Products} \quad \text{(k)}$$

As β-CD shows higher affinity on TiO_2 surface than dye molecules they can adsorb on TiO_2 surface, engage the active sites of TiO_2, and would capture the holes available on the active TiO_2 surface resulting in the formation of stable TiO_2-β-CD (b). The reaction (c) is the inclusion complex reaction of β-CD with AY99 dye molecules and it should be the key step in photocatalytic decoloration in TiO_2 suspension containing β-CD [24]. AY99 dye molecules form inclusion complex, resulting in indirect photodecoloration is to be the main reaction channel. AY99 dye molecules enter into β-CD cavity, which is linked to TiO_2 surface in equilibrium stage (d) and absorb light radiation followed by excitation (e). An electron is rapidly injected from the excited dye to the CB of TiO_2 (f) and the presence of oxygen leads to the formation of singlet oxygen (g). Another important radical in illumination of TiO_2-β-CD is the superoxide anion radical ($^{\bullet}O_2^-$) (h). The dye and dye cation radical then undergo degradation (i–k) [37].

In general, the lifetimes for the excited states of unreacted guests is prolonged when incorporated inside the cavity of CDs. Therefore, CD facilitates the electron injection from the excited dyes to the TiO_2 CB and thereby enhances the photodecoloration [37,38].

4. Conclusion

In this work, we carried out a detailed study of the effect of β-CD on the photodegradation of AY99 dye in TiO_2 suspension. XRD analysis reveals that TiO_2 conserved their anatase crystal features during the irradiation. Addition of β-CD does not cause any shift in peak position of that of TiO_2 phase. The results also demonstrated that the anatase TiO_2 conserved their anatase crystal features. UV–Visible diffuse reflectance spectra demonstrated that β-CD addition leads to a significant effect on the optical characteristics of TiO_2. TiO_2-β-CD system has slightly higher absorption intensity in the visible region compared to the bare TiO_2 system. Hence, photodecoloration of AY99 dye in TiO_2-β-CD/visible light system exhibits better photocatalytic decoloration efficiency than that of TiO_2/visible light system. This work provides basic information on the promotion effects of β-CD on the photodegradability of TiO_2 on the dye in aqueous solution.

Acknowledgments

The authors thank the Management and the Principal of Ayya Nadar Janaki Ammal College, Sivakasi, Tamilnadu, India for providing necessary facilities. Authors also thank the University Grants Commission, New Delhi, for the financial support through UGC-Major Research Project Ref. [UGC - Ref. No.F. No. 38-22/2009 (SR) Dated: 19.12.2009]. The instrumentation centre, Ayya Nadar Janaki Ammal College, Sivakasi, Centre for Nanoscience and Nanotechnology, Bharathidasan University, Tiruchirappalli, and Department of Earthscience, Pondicherry University, Pondicherry are highly appreciated for recording the UV–Visible, FT-IR spectra, FESEM, and Powder XRD patterns, respectively.

References

[1] M.R. Hoffmann, S.T. Martin, W. Choi, D.W. Bahnemann, Environmental applications of semiconductor photocatalysis, Chem. Rev. 95 (1995) 69–96.

[2] K.F. Zhou, Y.H. Zhu, X.L. Yang, X. Jiang, C.Z. Li, Preparation of graphene–TiO_2 composites with enhanced photocatalytic activity, New J. Chem. 35 (2011) 353–359.

[3] Z.G. Xiong, L.L. Zhang, J.Z. Ma, X.S. Zhao, Photocatalytic degradation of dyes over graphene–gold nanocomposites under visible light irradiation, Chem. Commun. 46 (2010) 6099–6101.

[4] T. Wu, G. Liu, J. Zhao, H. Hidaka, N. Serpone, Photoassisted degradation of dye pollutants. self-photosensitized oxidative transformation of rhodamine B under visible light irradiation in aqueous TiO_2 dispersions, J. Phys. Chem. B 102 (1998) 5845–5851.

[5] K. Woan, G. Pyrgiotakis, W. Sigmund, Photocatalytic carbon-nanotube-TiO_2 composites, Adv. Mater. 21 (2009) 2233–2239.

[6] A.L. Linsebigler, G.Q. Lu, J.T. Yates, Photocatalysis on TiO_2 surfaces: Principles, mechanisms, and selected results, Chem. Rev. 95 (1995) 735–758.

[7] S.C. Liao, H.F. Lin, S.W. Hung, C.T. Hu, Dc thermal plasma synthesis and propertiesof zinc oxide nanorods, J. Vac. Sci. Technol. B 24 (2006) 1332–1335.

[8] T. Hirakawa, P.V. Kamat, Charge separation and catalytic activity of Ag@TiO_2 core−shell composite clusters under UV−irradiation, J. Am. Chem. Soc. 127 (2005) 3928–3934.

[9] D. Kannaiyan, E. Kim, N. Won, K.W. Kim, Y.H. Jang, M.A. Cha, On the synergistic coupling properties of composite CdS/TiO_2 nanoparticle arrays confined in nanopatterned hybrid thin films, J. Mater. Chem. 20 (2010) 677–682.

[10] S.H. Liu, L.X. Yang, S.H. Xu, S.L. Luo, Q.Y. Cai, Photocatalytic activities of C–N-doped TiO2 nanotube array/carbon nanorod composite, Electrochem. Commun. 11 (2009) 1748–1751.

[11] S. Fukuzumi, T. Kojima, Photofunctional nanomaterials composed of multiporphyrins and carbon-based π-electron acceptors, J. Mater. Chem. 18 (2008) 1427–1439.

[12] Q.P. Luo, X. Yu, B.X. Lei, H.Y. Chen, D.B. Kuang, C.Y. Su, Reduced graphene oxide-hierarchical ZnO hollow sphere composites with enhanced photocurrent and photocatalytic activity, J. Phys. Chem. C 116 (2012) 8111–8117.

[13] Y. Willner, A.J. Eichen, Titanium dioxide and cadmium sulfide colloids stabilized by β-cyclodextrins: tailored semiconductor-receptor systems as a means to control interfacial electron-transfer processes, J. Am. Chem. Soc. 109 (1987) 6862–6863.

[14] Y. Willner, A.J. Eichen, Tailored semiconductor-receptor colloids: Improved photosensitized H_2 evolution from water with TiO_2-β-cyclodextrin colloids, J. Am. Chem. Soc. 111 (1989) 1884–1886.

[15] I. Willner, Y. Eichen, B. Willner, Supramolecular semiconductor receptor assemblies: Improved electron transfer at TiO_2-β-cyclodextrin colloids interfaces, Res. Chem. Intermed. 20 (1994) 681–700.

[16] T. Tachikawa, S. Tojo, M. Fujitsuka, T. Majima, One-electron oxidation pathways during β-cyclodextrin-modified TiO_2 photocatalytic reactions, Chem. Eur. J. 12 (2006) 7585–7594.

[17] N.M. Dimitrijevic, Z.V. Saponjic, D.M. Bartels, M.C. Thurnauer, D.M. Tiede, T. Rajh, Revealing the nature of trapping sites in nanocrystalline titanium dioxide by selective surface modification, J. Phys. Chem. B 107 (2003) 7368–7375.

[18] N.M. Dimitrijevic, T. Rajh, Z.V. Saponjic, L. de la Garza, D.M. Tiede, Light-induced charge separation and redox chemistry at the surface of TiO2/host-guest hybrid nanoparticles, J. Phys. Chem. B108 (2004) 9105–9110.

[19] J. Feng, A. Miedaner, P. Ahrenkiel, M.E. Himmel, C. Curtis, D. Ginley, Self-assembly of photoactive TiO_2-cyclodextrin wires, J. Am. Chem. Soc. 127 (2005) 14967–14968.

[20] M. Du, J. Feng, S.B. Zhang, Photo-oxidation of polyhydroxyl molecules on TiO_2 surfaces: From hole scavenging to light-induced self-assembly of TiO_2-cyclodextrin wires, Phys. Rev. Lett. 98 (2007) 066102-1–066102-4.

[21] S. Anandan, M. Yoon, Photocatalytic degradation of Nile red using TiO_2-β-cyclodextrin colloids, Catal. Commun. 5 (2004) 271–275.

[22] P. Lu, F. Wu, N.S. Deng, Enhancement of TiO_2 photocatalytic redox ability by β-cyclodextrin in suspended solutions, Appl. Catal. B 53 (2004) 87–93.

[23] G.H. Wang, F. Wu, X. Zhang, M.D. Luo, N.S. Deng, Enhanced TiO_2 photocatalytic degradation of bisphenol A by β-cyclodextrin in suspended solutions, J. Photochem. Photobiol. A 179 (2006) 49–56.

[24] X. Zhang, F. Wu, Z. Wang, Y. Guo, N.S. Deng, Photocatalytic degradation of 4,4′-biphenol in TiO_2 suspension in the presence of cyclodextrins: A trinity integrated mechanism, J. Mol. Catal. A 301 (2009) 134–139.

[25] X. Zhang, Z. Yang, X. Li, N. Deng, S. Qiana, β-Cyclodextrin's orientation onto TiO2 and its paradoxical role in guest's photodegradation, Chem. Commun. 49 (2013) 825–827.

[26] X. Zhang, X. Li, N. Deng, Enhanced and selective degradation of pollutants over cyclodextrin/TiO2 under visible light irradiation, Ind. Eng. Chem. Res. 51 (2012) 704–709.

[27] F.P.V.D. Zee, S. Villaverde, Combined anaerobicaerobic treatment of azo dyes — A short review of bioreactor studies, Water Res. 39 (2005) 1425–1440.

[28] N. Mariana, I. Siminiceanu, A. Yediler, A. Kettrup, Kinetics of decolorization and mineralization of reactive azo dyes in aqueous solution by UV/H_2O_2 oxidation, Dyes Pigm. 53 (2002) 93–99.

[29] P. Pekakis, N.P. Xekoukoulotakis, D. Mantzavinos, Treatment of textile dye house wastewater by photocatalysis, Water Res. 40 (2006) 1276–1286.

[30] C.C. Chen, H.J. Fan, C.Y. Jang, J.L. Jan, H.D. Lin, C.S. Lu, Photooxidative *N*-de-methylation of crystal violet dye in aqueous nano-TiO_2 dispersions under visible light irradiation, J. Photochem. Photobiol. A 184 (2006) 147–154.

[31] J.W. Lee, S.P. Choi, R. Thiruvenkatachari, W.G. Shim, H. Moon, Evaluation of the performance of adsorption and coagulation processes for the maximum removal of reactive dyes, Dyes Pigm. 69 (2006) 196–203.

[32] S. Sharma, S. Pathak, K.P. Sharma, Toxicity of the azo dye methyl red to the organisms in microsystems, with special reference to the guppy (Poecillia reticulate Peters), Bull. Environ. Contam. Toxicol. 70 (2003) 753–760.

[33] C.Y. Chen, Photocatalytic degradation of azo dye reactive orange 16 by TiO_2, Water Air Soil Pollut. 202 (2009) 335–342.

[34] Z. Zainal, L.K. Hui, M.Z. Hussein, Y.H. Taufiq-Yap, A.H. Abdullah, I. Ramli, Removal of dyes using immobilized titanium dioxide illuminated by fluorescent lamps, J. Hazard. Mater. B 125 (2005) 113–120.

[35] G. Alhakimi, L.H. Studnicki, M. Al-Ghazali, Photocatalytic destruction of potassium hydrogen phthalate using TiO_2 and sunlight: Application for the treatment of industrial wastewater, J. Photochem. Photobiol. A 154 (2003) 219–228.

[36] X. Zhang, F. Wu, N. Deng, Degradation of paracetamol in self assembly β-cyclodextrin/TiO_2 suspension under visible irradiation, Catal. Commun. 11 (2010) 422–425.

[37] X. Zhang, F. Wu, N.S. Deng, Efficient photodegradation of dyes using light-induced self assembly TiO_2/β-cyclodextrin hybrid nanoparticles under visible light irradiation, J. Hazard. Mater. 185 (2011) 117–123.

[38] P. Velusamy, S. Pitchaimuthu, S. Rajalakshmi, N. Kannan, Modification of the photocatalytic activity of TiO_2 by β-cyclodextrin in decoloration of ethyl violet dye, J. Adv. Res. (accepted for publication) doi: 10.1016/j.jare.2012.10.001.

[39] P. Velusamy, K. Pitchumani, C. Srinivasan, Selectivity in the bromination of aniline and N-substituted anilines encapsulated in β-Cyclodextrin, Tetrahedron 52 (1996) 3487–3496.

[40] N. Daneshvar, D. Salari, A.R. Khataee, Photocatalytic degradation of azo dye acid red 14 in water: investigation of the effect of operational parameters, J. Photochem. Photobiol. A 157 (2003) 111–116.
[41] Y.L. Song, J.T. Li, B. Bai, TiO_2-assisted photodegradation of direct blue 78 in aqueous solution in sunlight, Water Air Soil Pollut. 213 (2010) 311–317.
[42] R. Camarillo, J. Rincon, Photocatalytic discoloration of dyes: Relation between effect of operating parameters and dye structure, Chem. Eng. Technol. 34 (2011) 1675–1684.
[43] N. Sobana, K. Selvam, M. Swaminathan, Optimization of photocatalytic degradation conditions of direct red 23 using nano-Ag doped TiO_2, Sep. Purif. Technol. 62 (2008) 648–653.
[44] H. Chun, W. Yizhong, T. Hongxiao, Preparation and characterization of surface bond-conjugated TiO_2/SiO_2 and photocatalysis for azo dyes, Appl. Catal. B 30 (2001) 277–285.
[45] A. Zertal, D.M. Gabor, M.A. Malouki, T. Sehili, P. Boule, Photocatalytic transformation of 4-chloro-2-methylphenoxyacetic acid (MCPA) on several kinds of TiO_2, Appl. Catal. B 49 (2004) 83–89.
[46] M. Kamiya, K. Kameyama, S. Ishiwata, Effects of cyclodextrins on photodegradation of organophosphorus pesticides in humic water, Chemosphere 42 (2001) 251–255.